© 2021. Published by The Company of Biologists Ltd | Journal of Cell Science (2021) 134, jcs254714. doi:10.1242/jcs.254714

RESEARCH ARTICLE

The methanol sensor Wsc1 and MAPK Mpk1 suppress degradation of methanol-induced peroxisomes in methylotrophic yeast

Shin Ohsawa[1,*], Koichi Inoue[1,*], Takahiro Isoda[1], Masahide Oku[2], Hiroya Yurimoto[1] and Yasuyoshi Sakai[1,3,‡]

ABSTRACT

In nature, methanol is produced during the hydrolysis of pectin in plant cell walls. Methanol on plant leaves shows circadian dynamics, to which methanol-utilizing phyllosphere microorganisms adapt. In the methylotrophic yeast *Komagataella phaffii* (Kp; also known as *Pichia pastoris*), the plasma membrane protein KpWsc1 senses environmental methanol concentrations and transmits this information to induce the expression of genes for methanol metabolism and the formation of huge peroxisomes. In this study, we show that KpWsc1 and its downstream MAPK, KpMpk1, negatively regulate pexophagy in the presence of methanol concentrations greater than 0.15%. Although KpMpk1 was not necessary for expression of methanol-inducible genes and peroxisome biogenesis, KpMpk1, the transcription factor KpRlm1 and phosphatases were found to suppress pexophagy by controlling phosphorylation of KpAtg30, the key factor in regulation of pexophagy. We reveal at the molecular level how the single methanol sensor KpWsc1 commits the cell to peroxisome synthesis and degradation according to the methanol concentration, and we discuss the physiological significance of regulating pexophagy for survival in the phyllosphere.

This article has an associated First Person interview with Shin Ohsawa, joint first author of the paper.

KEY WORDS: Peroxisome, Autophagy, Mitogen-activated protein kinase, Organelle homeostasis, Pexophagy

INTRODUCTION

Autophagy refers to the degradation pathway of cellular components after transport into the vacuole and/or lysosome, and plays versatile physiological roles in unicellular and multicellular eukaryotes (Mizushima and Komatsu, 2011). Extensive studies have shown that selective autophagy of organelles employs 'receptor' proteins on the surface of the autophagy target organelles that recruit the Atg (autophagy-related) protein machinery for formation of autophagosomes (Xie and Klionsky, 2007). In the methylotrophic yeast *Komagataella phaffii* (Kp; also known as *Pichia pastoris*), which serves as a model organism for studying pexophagy (Pang et al., 2019; Sakai et al., 1998), KpAtg30 exerts its role by interacting with the peroxins KpPex3, KpPex14 and KpAtg37, which are necessary for peroxisome biogenesis, and the Atg proteins KpAtg8 and KpAtg11 (Burnett et al., 2015; Farré et al., 2013, 2008; Nazarko et al., 2014). The interaction between KpAtg30 and KpAtg11 requires phosphorylation of KpAtg30 by the kinase KpHrr25, which serves as a cue for pexophagy induction (Zientara-Rytter et al., 2018). In the yeast *Saccharomyces cerevisiae* (Sc), ScHrr25 and the pexophagy receptor protein ScAtg36 function in a similar way (Tanaka et al., 2014).

In contrast to the molecular mechanism and machinery of autophagy, the physiological roles of pexophagy in yeasts and fungi have been less studied, with the exception of plant pathogenicity (Asakura et al., 2009; Oku and Sakai, 2016; Oku et al., 2014). We have previously reported that by adapting to the methanol concentration in the environment, the methylotrophic yeasts *Candida boidinii* and *K. phaffii* proliferate slowly on plant leaves, undergoing 3–4 cell divisions in 7–10 days (Kawaguchi et al., 2011). The methanol concentration on plant leaves exhibits diurnal fluctuations, with high concentrations in the dark period and low concentrations in the light period. When the methanol concentration is high in the dark period, peroxisomes containing major methanol-utilizing enzymes are highly induced. In contrast, when the methanol concentration becomes low in the light period, peroxisomes are degraded by pexophagy (Kawaguchi et al., 2011). The induction of peroxisomes and methanol-utilizing enzymes, as well as Atg30-dependent pexophagy, are necessary for methylotrophic yeast cells to proliferate on plant leaves, indicating the essential role of peroxisome homeostasis and its regulation in cellular survival on plant leaves (Kawaguchi et al., 2011).

We have also previously reported that the cell-surface proteins KpWsc1 and KpWsc3, homologs of ScWsc1 in *S. cerevisiae*, are responsible for sensing the concentration of environmental methanol and regulating methanol-inducible gene expression (i.e. genes encoding proteins involved in peroxisome synthesis and methanol-metabolizing enzymes) in *K. phaffii* (Ohsawa et al., 2017). ScWsc1 is a glycosylphosphatidylinositol (GPI)-anchored plasma membrane protein that senses the perturbation of cell wall integrity (CWI) (Dupres et al., 2009; Lodder et al., 1999) and initiates a phosphorylation cascade (MAPK cascade) leading to the activation of a MAPK (ScMpk1, also known as Slt2) to activate expression of cell wall-related genes, such as those related to glucan synthesis (Levin, 2011; Rodicio and Heinisch, 2010). Our previous study with *K. phaffii* showed that knockout of *KpWSC1* leads to unbalanced methanol metabolism, resulting in formaldehyde accumulation and retardation of cell growth (Ohsawa et al., 2017). KpWsc1 and its downstream factor KpRom2 are involved not only in methanol-induced gene expression, but also in the high-temperature stress

[1]Division of Applied Life Sciences, Graduate School of Agriculture, Kyoto University, Kitashirakawa-Oiwake, Sakyo-ku, Kyoto 606-8502, Japan. [2]Department of Bioscience and Biotechnology, Faculty of Bioenvironmental Science, Kyoto University of Advanced Science, Sogabecho Nanjo Otani, Kameoka 621-8555, Japan. [3]Research Unit for Physiological Chemistry, the Center for the Promotion of Interdisciplinary Education and Research, Kyoto University, Kitashirakawa-Oiwake, Sakyo-ku, Kyoto 606-8502, Japan.
*These authors contributed equally to this work

‡Author for correspondence (sakai.yasuyoshi.8x@kyoto-u.ac.jp)

M.O., 0000-0001-5991-6281; H.Y., 0000-0001-7506-6184; Y.S., 0000-0002-9831-3085

Handling Editor: Tamotsu Yoshimori
Received 21 September 2020; Accepted 17 March 2021

Journal of Cell Science

Journal of Cell Science (2021) 134, jcs254714. doi:10.1242/jcs.254714

response in *K. phaffii* (Ohsawa et al., 2017), which is similar to the CWI pathway in *S. cerevisiae*. Signaling of the two pathways could be dissected using mutations in KpWsc1, and the two pathways were thus shown to be independent of each other (Ohsawa et al., 2017).

In the present study, we examined how the environmental methanol concentration affects and regulates pexophagy, that is, degradation of methanol-induced peroxisomes. We found that the presence of methanol, which was sensed by KpWsc1, activated the downstream MAPK and suppressed pexophagy. Cellular sensing of nutrient concentrations has been shown to play a critical role in maintaining organellar homeostasis. The physiological significance of a regulatory mechanism of selective autophagy in cellular survival in nature is discussed.

RESULTS

Pexophagy during methanol consumption in batch-cultured growth of *K. phaffii*

In order to compare pexophagy between two different strains of *K. phaffii* in response to the methanol concentration, we used a Beppu flask in which the two compartments of the flask are separated by a membrane (pore size 0.22 µm) that allows medium components, including methanol, to pass through and be maintained at the same level, but does not allow yeast cells to mix (Fig. 1A).

Pexophagy was compared between the wild-type strain and the pexophagy-deficient strain *Kpatg30*Δ. The wild-type cells consumed methanol, proliferated and reached stationary phase after ∼20 h of cultivation, with complete consumption of methanol (Fig. S1A). Pexophagy was monitored by observing cleavage of a YFP-fused form of the peroxisomal membrane protein KpPex11 (Pex11–YFP), which yields a YFP fragment resistant to vacuolar proteases. The cleaved YFP band appeared after ∼16 h (0.15% methanol) to 18 h (0.04% methanol), and after depletion of methanol at 20 h, the band of cleaved YFP became more intense (Fig. S1B).

The pexophagy process of the *Kpatg30*Δ strain inoculated in the other compartment of the Beppu flask was compared with that of the wild-type strain. KpAtg30 is a pexophagy factor acting as a receptor on the peroxisome membrane (Farré et al., 2008). Comparison of the wild-type and *Kpatg30*Δ strains in the Beppu flask revealed that the methanol concentrations in the two compartments of the flask showed the same kinetics of methanol consumption and that both strains showed similar growth curves (Fig. S1A). As expected, cleavage of Pex11–YFP was inhibited in the *Kpatg30*Δ strain (Fig. S1B). After 20 h, the wild-type strain expressing a peroxisome-targeted CFP (CFP–SKL) exhibited a diffuse CFP signal pattern in the vacuolar lumen (Fig. S1C, Table S4). In contrast, the percentage of cells with a diffuse pattern of CFP fluorescence in the vacuole was remarkably reduced in the *Kpatg30*Δ strain. These results collectively indicate that Atg30-dependent pexophagy is induced at the late exponential to early stationary phase (16–18 h) in batch cultures of *K. phaffii* when the methanol concentration falls below 0.15%.

Methanol sensed by Wsc1 negatively regulates pexophagy

Next, we compared pexophagy between the wild-type and *Kpwsc1*Δ strains. In a previous study, we have shown that the *Kpwsc1*Δ strain is impaired in sensing the environmental methanol concentration (Ohsawa et al., 2017). Although the *Kpwsc1*Δ strain showed a decreased growth yield in a Beppu flask, the two strains showed similar growth curves (Fig. 1A). Accumulation of formaldehyde in the *Kpwsc1*Δ strain, which was observed when this strain was cultivated alone, was avoided due to consumption of formaldehyde by the wild-type strain.

The *Kpwsc1*Δ strain exhibited an earlier onset of pexophagy than the wild-type strain. In the *Kpwsc1*Δ strain, higher ratios of the cleaved YFP band to the full length Pex11–YFP were observed as early as 12 h of cultivation (Fig. 1B), when more than 0.25% methanol was still present in the medium. As judged from the

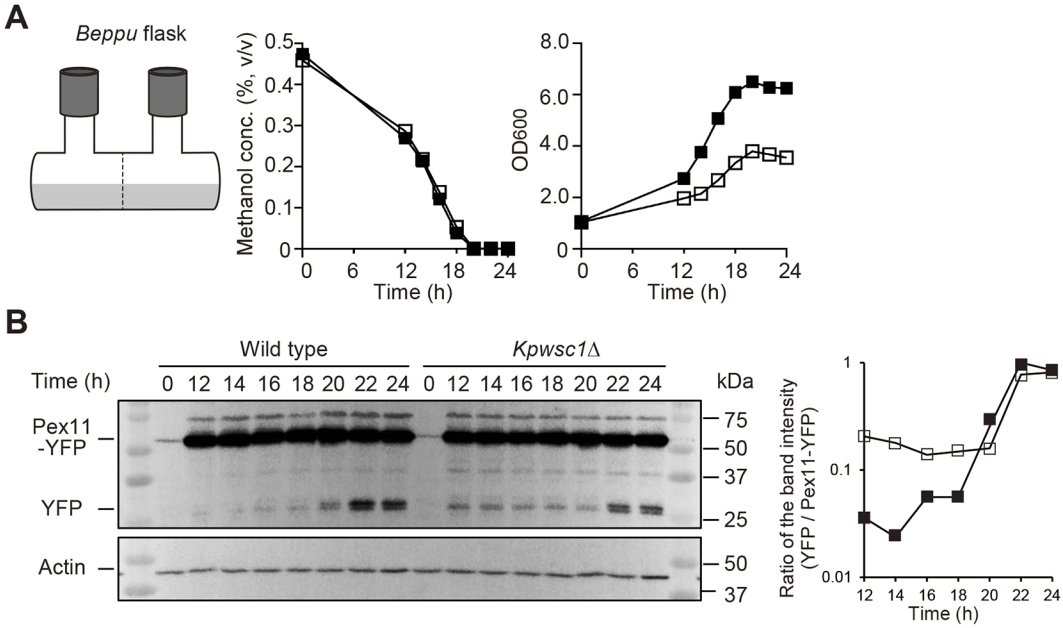

Fig. 1. KpAtg30-dependent pexophagy is enhanced in the *Kpwsc1*Δ strain during batch culture on methanol in a Beppu flask. (A) Illustration of a Beppu flask (left; dashed line, membrane), kinetics of methanol consumption (middle) and growth ($OD_{600\ nm}$) of the wild-type and *Kpwsc1*Δ strains (right) in two chambers of the Beppu flask. (B) Immunoblot analysis of KpPex11–YFP expressed in the wild-type and *Kpwsc1*Δ strains (left). Anti-β-actin antibody was used for the actin loading control. Quantitative analysis of the intensity of YFP-band relative to that of KpPex11–YFP band (right). Data shown are mean values from single experiments performed in triplicate and are representative of three independent experiments. Closed square, wild-type strain; open square, *Kpwsc1*Δ strain.

Journal of Cell Science (2021) 134, jcs254714. doi:10.1242/jcs.254714

difference in the timing of pexophagy induction between the wild-type and *Kpwsc1*Δ strains (Fig. 1B), KpWsc1 is considered to suppress the degradation of methanol-induced peroxisomes in the presence of more than 0.15% methanol.

Next, we compared macropexophagy between the wild-type and *Kpwsc1*Δ cells by shifting methanol-induced cells to ethanol-containing medium. Macropexophagy was monitored by observing cleavage of YFP-fused KpAtg8 (Atg8–YFP). As shown in Fig. S2, we did not observe enhancement of pexophagy in the *Kpwsc1*Δ mutant. These results suggest that KpWsc1 is not involved in regulation of ethanol-induced macropexophagy.

Depletion of KpWsc1 enhances phosphorylation of KpAtg30

To elucidate the molecular mechanism of pexophagy suppression by methanol and its sensor KpWsc1, we next analyzed phosphorylation of KpAtg30, which induces pexophagosome formation at the peroxisomal surface (Farré et al., 2008). In the following experiments, we used *Kpatg11*Δ as the background strain to observe the phosphorylation level of HA-tagged KpAtg30 (KpAtg30–3×HA). In the *Kpatg11*Δ strain, degradation of KpAtg30–3×HA through pexophagy was blocked, and phosphorylated bands of KpAtg30–3×HA were readily visible. In the periodically sampled lysate of the *Kpatg11*Δ strain, the phosphorylation level of KpAtg30–3×HA was found to increase gradually with cultivation time, giving multiple bands of less mobility than the non-phosphorylated form (Fig. 2A). Next, we examined whether KpWsc1 depletion affects the phosphorylation level of KpAtg30–3×HA during growth on methanol. KpAtg30–3×HA in the *Kpwsc1*Δ*atg11*Δ strain was found to be more highly phosphorylated in samples from a 12 h culture and thereafter than that in the *Kpatg11*Δ strain (Fig. 2A), consistent with the observed enhancement of pexophagy by depletion of KpWsc1 (Fig. 1B).

In our previous study, two variants of KpWsc1 mutated at the tyrosine 53 residue were found to have distinct phenotypes: the KpWsc1 Y53A mutation (but not the Y53F mutation) results in impaired methanol-inducible gene expression, and the KpWsc1 Y53F mutation (but not the Y53A mutation) renders the cells more susceptible to high-temperature stress (Ohsawa et al., 2017). The phosphorylation levels of KpAtg30–3×HA in strains carrying these KpWsc1 variants were analyzed, and the wild-type KpWsc1 and its Y53A variant reverted the hyper-phosphorylation phenotype of KpAtg30–3×HA in the *Kpwsc1*Δ*atg11*Δ strain. In contrast, the Y53F variant could not (Fig. 2B). These results indicate that signaling mediated by KpWsc1, which is similar to the high-temperature stress response, was required for suppression of KpAtg30 phosphorylation. In line with this result, another KpWsc1 mutant (310–316Δ) incapable of interacting with KpRom2 (a signaling factor downstream of Wsc1) failed to revert the hyper-phosphorylation phenotype in the *Kpwsc1*Δ *atg11*Δ strain (Fig. 2C).

Among the identified *K. phaffii* Wsc proteins, KpWsc3 has also been found to be involved in methanol-inducible gene expression, but not in the high-temperature stress response (Ohsawa et al., 2017). Overexpression of KpWsc3–FLAG failed to revert the hyper-phosphorylation phenotype of *Kpwsc1*Δ*atg11*Δ, even though the protein expression level was higher than that of KpWsc1–FLAG (Fig. S3A). This reinforces the notion that KpWsc1-mediated pexophagy regulation that is distinct from the methanol-inducible gene expression pathway is responsible for suppression of KpAtg30 phosphorylation in *K. phaffii*.

In *S. cerevisiae*, the CWI pathway leads to phosphorylation and activation of the MAPK ScMpk1 by MAPK kinases (Irie et al., 1993; Lee et al., 1993). The *Kpmpk1*Δ strain showed normal growth on methanol, together with peroxisome proliferation. To assess the involvement of KpMpk1 in *K. phaffii,* the pexophagy process and phosphorylation of KpAtg30–3×HA was compared between *Kpmpk1*Δ and wild-type strains. We found an earlier onset of pexophagy in the *Kpmpk1*Δ strain cultured with the wild-type strain in a Beppu flask, similar to that observed in the *Kpwsc1*Δ strain (Fig. S3B), and depletion of KpMpk1 from the *Kpatg11*Δ strain further enhanced phosphorylation of KpAtg30-3xHA (Fig. 2D, lanes *Kpatg11*Δ and EV in *Kpmpk1*Δ*atg11*Δ). While the wild-type Mpk1 tagged with YFP was able to revert the hyper-phosphorylation phenotype of the *Kpmpk1*Δ*atg11*Δ strain, a KpMpk1 variant mutated in the conserved phosphorylation residues (TAYF mutant: T188 and Y190 residues replaced with alanine and phenylalanine, respectively) did not (Fig. 2D). These results strongly suggest that phosphorylated Mpk1 suppresses phosphorylation of KpAtg30 in the presence of methanol. Taken together with the data for the *Kpwsc1* mutants, we conclude that the MAPK pathway in *K. phaffii* under the control of KpWsc1, KpRom2 and KpMpk1, was responsible for suppression of KpAtg30 phosphorylation.

KpRlm1, but not KpSwi4, is involved in suppressing phosphorylation of KpAtg30 during methanol culture

In *S. cerevisiae*, ScMpk1 relays the CWI signaling cascade by phosphorylation of the transcriptional factors ScRlm1, ScSwi4 and ScSwi6, which are required for gene expression involved in cell wall synthesis (Levin, 2011; Watanabe et al., 1995). We tested whether these downstream transcription factors in *K. phaffii* were involved in phosphoregulation of KpAtg30. In the *K. phaffii* genome, we identified two putative genes encoding homologs of the above transcription factors, and named them *KpRLM1* and *KpSWI4*, based on sequence similarity. We disrupted these genes in the *K. phaffii atg11*Δ strain, yielding the *Kprlm1*Δ*atg11*Δ and *Kpswi4*Δ*atg11*Δ strains. KpAtg30–3×HA was highly phosphorylated in *Kprlm1*Δ*atg11*Δ cells, whereas the phosphorylation level of KpAtg30–3×HA in the *Kpswi4*Δ*atg11*Δ strain was comparable to that in the *Kpatg11*Δ strain (Fig. 3A). We also found that cleavage of Pex11–YFP was enhanced in the *Kprlm1*Δ strain at 18 and 22 h, when methanol still remained in the medium (Fig. S4). These results suggest that KpMpk1 suppresses phosphorylation of KpAtg30 by transcriptional control under KpRlm1, and not KpSwi4.

Identification of a putative phosphatase suppressing phosphorylation of Atg30

After screening for phosphatases regulated by KpRlm1, we found that the transcript levels of *KpMSG5* (XM_002492799.1) and *KpPTP2A* (XP_002491091.1; a paralog of *ScPTP2*) were reduced in the *Kprlm1*Δ strains (Fig. 3B), whereas the expression level of *KpPTP2B* (the other paralog of Sc*PTP2*) was independent of KpRlm1 (data not shown). Next, we investigated whether these phosphatases were involved in the suppression of Atg30 phosphorylation (Fig. 4A,B). Depletion of the KpPtp2A phosphatase in the *Kpatg11*Δ strain enhanced phosphorylation of KpAtg30–3×HA after 17 h growth on methanol, when methanol was still present in the medium, and the *Kpmsg5*Δ strain also showed slight enhancement of Atg30 phosphorylation. The *Kpptp2A*Δ*msg5*Δ*atg11*Δ strain exhibited higher phosphorylation levels than observed in other tested strains (Fig. 4C), although methanol still remained at higher concentrations with this triple disruption strain than other strains. These results indicate that the KpPtp2A and KpMsg5 phosphatases act downstream of KpRlm1 and have a role in the suppression of KpAtg30 phosphorylation in *K. phaffii*. Based on sequence similarity, both KpPtp2A and KpMsg5 are assumed to be tyrosine phosphatases,

Journal of Cell Science (2021) 134, jcs254714. doi:10.1242/jcs.254714

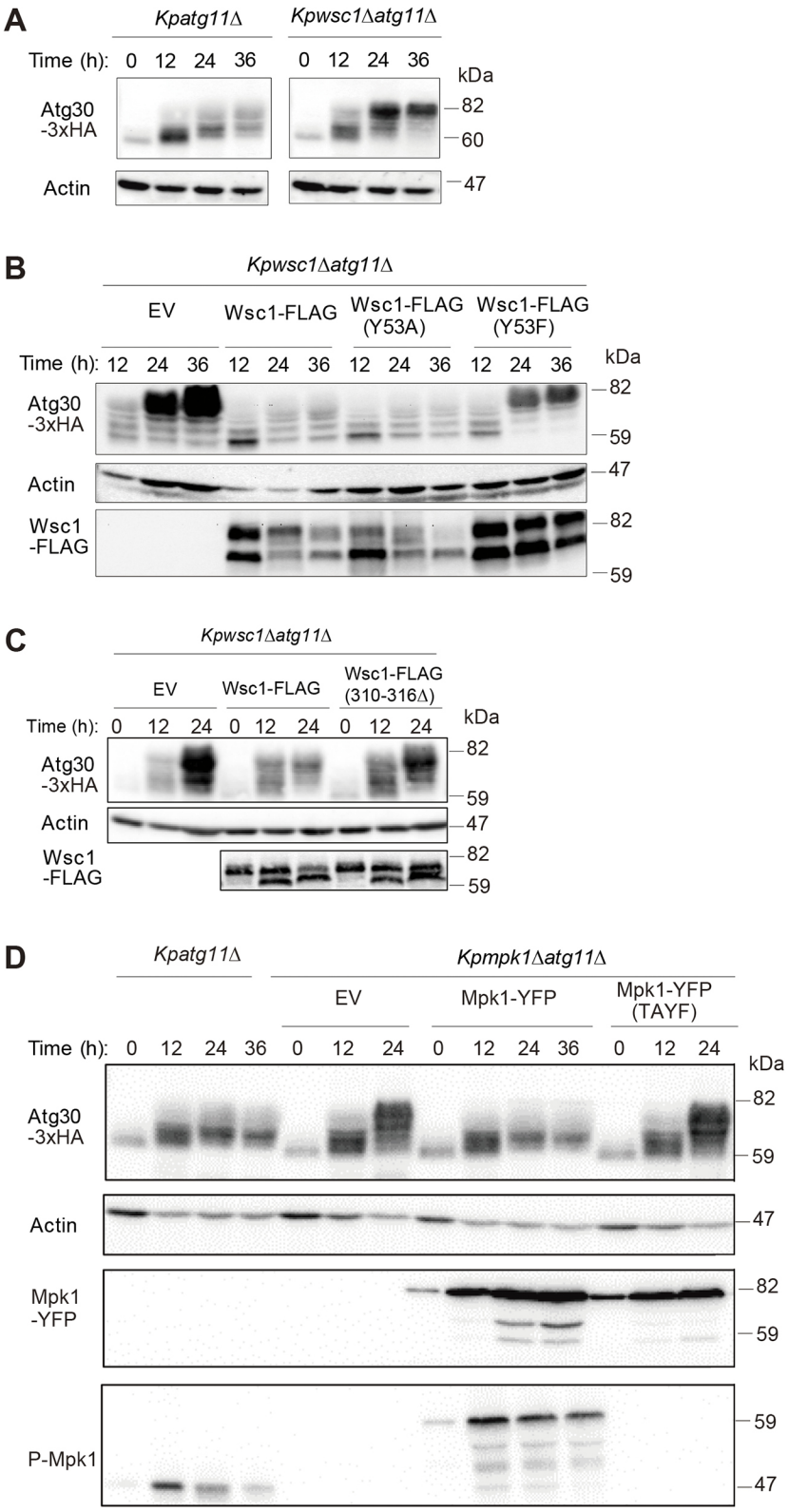

Fig. 2. The KpWsc1–MAPK pathway suppresses phosphorylation of KpAtg30–3×HA during methanol batch culture. (A) Immunoblotting of KpAtg30–3×HA in samples from methanol cultures of the indicated strains retrieved at the time points shown. Anti-HA antibody was used for the analysis. (B,C) Immunoblot analysis of KpAtg30–3×HA in *Kpwsc1Δatg11Δ* strains expressing empty vector (EV), KpWsc1–FLAG or the indicated KpWsc1–FLAG variants. The protein expression levels of KpWsc1–FLAG were visualized using anti-FLAG antibody reactive to FLAG and are shown in the bottom panel. (D) Immunoblot analysis of KpAtg30–3×HA in the *Kpatg11Δ* strain and in the *Kpmpk1Δatg11Δ* strain with empty vector (EV) or the indicated KpMpk1–YFP variants. The total protein expression levels of KpMpk1–YFP were compared using an anti-GFP antibody and the phosphorylated Mpk1 (P-Mpk1) was detected with using an anti-phospho-MAPK antibody. In A–D, anti-β-actin antibody was used for the actin loading control. Blots are representative of three experiments.

suggesting that these phosphatases do not act at serine 71 and serine 112 residues of KpAtg30, which are known to be important for binding of Atg8 and Atg11, respectively (Farré et al., 2013).

DISCUSSION

We have previously reported that KpWsc1 senses the environmental methanol concentration and transmits the signal to ensure an appropriate level of methanol-induced gene expression (Ohsawa et al., 2017). KpWsc1 gives maximum transcription output for peroxisome synthesis at methanol concentrations in the range of 0.05–0.1% (Ohsawa et al., 2017). In the phyllosphere, methylotrophic yeasts have been observed to respond to diurnal fluctuations of methanol (~0–0.3%), alternating peroxisome synthesis and degradation in response to these changes (Kawaguchi et al., 2011).

Journal of Cell Science (2021) 134, jcs254714. doi:10.1242/jcs.254714

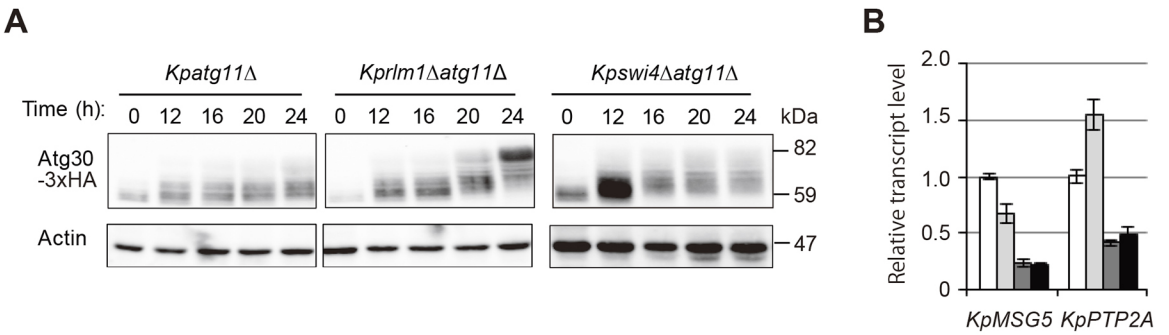

Fig. 3. Downstream factors of the KpWsc1–MAPK pathway suppress phosphorylation of KpAtg30 during methanol batch culture. (A) Immunoblot analysis of KpAtg30–3×HA in the indicated strains cultured as described in Fig. 2A. The blots shown are representative of three experiments. Anti-β-actin antibody was used for the actin loading control. (B) The mRNA levels of *KpMSG5* and *KpPTP2A* in the designated methanol-grown strains were compared using the transcript of *KpACT1* as the control. White, wild-type strain after 16 h cultivation; light gray, wild-type strain after 24 h cultivation; dark gray, *Kprlm1*Δ strain after 16 h cultivation; black, *Kprlm*Δ strain after 24 h cultivation. Data are mean±s.d. of three independent experiments.

In this study, the methanol-sensing molecule KpWsc1 was found to regulate not only the level of peroxisome synthesis, but also pexophagy according to the methanol concentration by two distinct signaling pathways.

KpWsc1 has previously been found to initiate dual signaling pathways: one leading to expression of methanol-inducible genes and peroxisome biogenesis, and the other dictating the high-temperature stress response, similar to the *S. cerevisiae* CWI pathway (Ohsawa et al., 2017). These two pathways have been clearly distinguished by mutations at the tyrosine 53 residue of KpWsc1. KpWsc1 Y53A inhibits methanol-inducible gene expression but does not inhibit the high-temperature stress response, and KpWsc1 Y53F has the opposite effect. Our present results demonstrate that suppression of pexophagy and KpAtg30 phosphorylation were abolished by the KpWsc1 Y53F mutation but not by the KpWsc1 Y53A mutation. Therefore, KpWsc1 determines synthesis or degradation of peroxisomes depending on the environmental methanol concentration (Fig. 5). Molecules downstream of KpWsc1, namely KpRom2, KpMpk1 and the transcription factor KpRlm1, were also shown to regulate the phosphorylation level of KpAtg30 (Fig. 2B–D, Figs 3,5). By analogy with the *S. cerevisiae* CWI pathway, we speculate that *K. phaffii* homologs of Rho1, Pkc1, and the MAP kinase cascade (including the MAPK kinase kinase, the MAPK kinase and the MAPK KpMpk1) are involved in suppression of pexophagy and that the methanol concentration input signal branches out to two pathways: methanol-inducible gene expression (peroxisome synthesis) through transcriptional factors (such as KpMxr1, KpTrm1 and KpMit1) (Lin-Cereghino et al., 2006; Ohsawa et al., 2018, 2017; Parua et al., 2012; Sahu et al., 2014; Wang et al., 2016) and suppression of pexophagy through

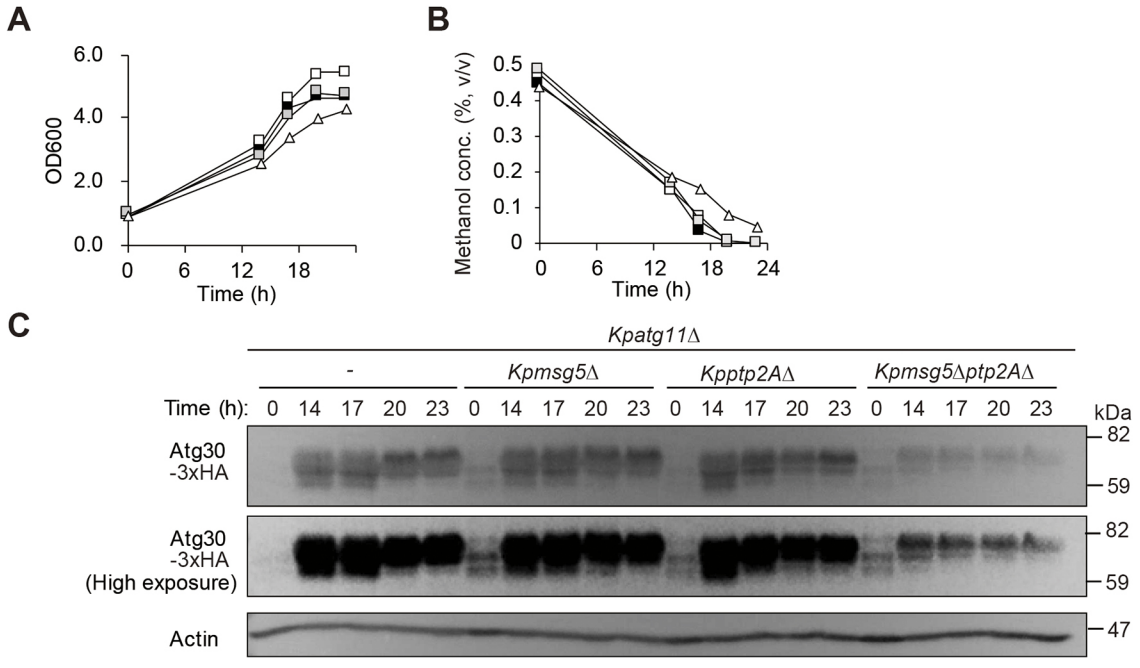

Fig. 4. Phosphorylation levels of KpAtg30–3×HA in *Kpmsg5*Δ, *Kpptp2A*Δ and *Kpmsg5*Δ*ptp2A*Δ strains expressing Atg30–3×HA. (A–C) The *Kpatg11*Δ strain was used as the background strain. (A) Growth ($OD_{600\ nm}$) on 0.5% methanol medium. (B) Methanol concentration in the medium over time. Closed square, *Kpatg11*Δ strain; open square, *Kpmsg5*Δ*atg11*Δ strain; gray square, *Kpptp2A*Δ*atg11*Δ strain; open triangle, *Kpmsg5*Δ*ptp2A*Δ*atg11*Δ strain. Data shown are from a single experiment, peformed in triplicate, that is representative of three independent experiments. (C) Immunoblot analysis of KpAtg30–3×HA in the indicated strains cultured as described in Fig. 2A. Anti-β-actin antibody was used for the actin loading control. Blots shown are representative of three experiments.

Journal of Cell Science (2021) 134, jcs254714. doi:10.1242/jcs.254714

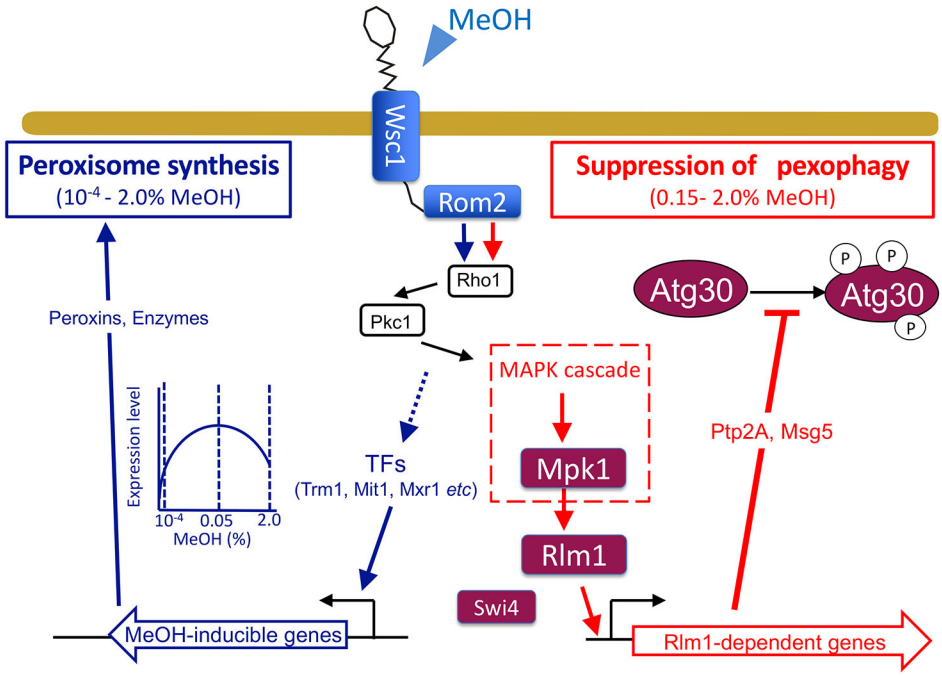

Fig. 5. Methanol-sensing by the KpWsc1–KpMpk1 pathway suppresses pexophagy in *K. phaffii*. According to previous studies, KpWsc1 senses methanol (MeOH) concentrations in the range of 1×10^{-4}–2.0% (Takeya et al., 2018), and transmits the signal via KpRom2 to transcriptional factors (TFs), including KpMxr1, KpTrm1 and KpMit1 (Lin-Cereghino et al., 2006; Ohsawa et al., 2018, 2017; Parua et al., 2012; Sahu et al., 2014; Wang et al., 2016), that are necessary for induction of methanol-inducible genes encoding proteins involved in peroxisome biogenesis (peroxins) and methanol-metabolizing enzymes. KpWsc1-dependent methanol-induced gene expression is maximal at 0.05–0.1% methanol. Since induction of peroxisomes is normal in *Kpmpk1*Δ cells, methanol-induced gene expression does not require KpMpk1. In contrast, suppression of pexophagy in the presence of methanol (0.15–2.0%) requires KpMpk1 and the downstream transcriptional factor, KpRlm1, a pathway that resembles the CWI pathway in *S. cerevisiae*. KpSwi4 is not involved in the process. KpRlm1-dependent expression of the KpPtp2A phosphatase regulates pexophagy, together with KpMsg5 phosphatase, through the phosphorylation (P) level of KpAtg30. The possible involvement of KpRho1, KpPkc1 and the MAPK cascade is shown. The signal transmission is assumed to diverge at some point upstream of KpMpk1.

phospho-regulation of KpAtg30 (Fig. 5). The phosphatase KpPtp2A was also involved in phosphoregulation of KpAtg30, although we could not confirm its direct phosphatase action *in vitro*.

While this study shows that the KpWsc1–MAPK pathway negatively regulates pexophagy in *K. phaffii*, in the past the MAPK pathway has been reported to support pexophagy and mitophagy in a positive manner (Manjithaya et al., 2010; Mao et al., 2011). Although KpAtg30 and ScAtg36 are both receptor proteins for pexophagy, they are not homologs (Farré et al., 2008; Motley et al., 2012). The discrepancy may be due in part to the differences in pexophagy regulation and the molecular machinery between *K. phaffii* and *S. cerevisiae*. Methanol-induced peroxisomes in *K. phaffii* are larger than oleate-induced peroxisomes of *K. phaffii* and *S. cerevisiae*. Indeed, the peroxisome size has been reported to determine the requirement for Atg proteins in *K. phaffii* (Nazarko et al., 2009).

Previous reports have suggested the involvement of the MAPKs ScMpk1 and ScHog1 and their mammalian homologs the p38 MAPKs in regulation of mitophagy and pexophagy (Meijer and Codogno, 2006) (Manjithaya et al., 2010). Overexpression of ScMpk1 inhibits pexophagy in wild-type cells, but its moderate expression accelerates pexophagy (Manjithaya et al., 2010). However, because the input signal and/or environmental stimuli upstream of the MAPK are not known, the physiological impact of MAPKs on the regulation of autophagy is not understood well. Yeast pexophagy has been followed after a shift from peroxisome-proliferating medium (methanol or oleate medium) to glucose or ethanol medium, in which peroxisomes are not required for metabolism, or to nitrogen-starvation conditions. Since such drastic changes of the medium could trigger multiple input signals simultaneously, their complexity has made the analyses of signaling pathways and interpretation of data difficult. In the present study, we were able to focus on one single environmental input, methanol concentration, and analyzed the intracellular signaling pathway. Higher methanol concentrations (0.15–2.0%) were found to suppress pexophagy. Surprisingly, the single sensor molecule KpWsc1 transmitted the methanol concentration input signal and regulated not only peroxisome synthesis, but also pexophagy. This result provides a perspective on the molecular mechanism of organellar homeostasis in response to an environmental cue.

During batch culture of *K. phaffii*, the methanol concentration decreased with cultivation time, during which growing cells sense methanol via KpWsc1 and regulate the expression of genes encoding methanol-metabolizing enzymes (Ohsawa et al., 2017). In our previous study of *C. boidinii* proliferating on plant leaves, we observed that the processing of GFP–Atg8, which is dependent Atg1 but not on Atg30, occurs throughout the daily dark–light cycle. Conversely, Atg30-dependent pexophagy was only observed in the light period. The methanol concentrations at late exponential phase (after 16 h) are considered to resemble the plant leaf environment in the light period, where the methanol concentration decreases to 0–0.15%. We think that the molecular mechanism of negative regulation of selective autophagy – pexophagy during bulk autophagic conditions – plays a critical role by optimizing the quantity of peroxisomes as a survival strategy in the phyllosphere. Further physiological understanding at the molecular level will deepen our insights into the survival strategies of microbes in nature.

Journal of Cell Science (2021) 134, jcs254714. doi:10.1242/jcs.254714

MATERIALS AND METHODS

Strains and medium

Escherichia coli DH10B (Takara Bio, Otsu, Japan) was used as a host strain for plasmid DNA propagation. *E. coli* cells were grown in LB medium (1% tryptone, 0.5% yeast extract, 0.5% NaCl) at 37°C.

The yeast strains used in this study are listed in Table S1. *K. phaffii* cells were grown on YPD (1% yeast extract, 2% peptone, 2% glucose) or YNB medium (0.67% yeast nitrogen base without amino acids). In the YNB medium, 2% (w/v) glucose (glucose medium) or 0.5% (v/v) methanol (methanol medium) were used as the carbon sources. Appropriate amino acids (100 µg/ml) were added to the synthetic media. All of the components other than the carbon sources used in these media were purchased from Difco Becton Dickinson (Franklin Lakes, NJ, USA). The growth of the yeast was monitored by the optical density (OD) at 600 nm ($OD_{600\ nm}$).

Plasmid construction and gene disruption

The oligonucleotide primers used in this study are listed in Table S3. The plasmids used in this study are listed in Table S2. A deletion cassette for the *KpATG11* gene was constructed as follows: primer pairs EcoRI-PpATG11-1-F/PpATG11-1-R and PpATG11-2-F/BamHI-PpATG11-2-R were used to amplify 1.0 kb fragments using genomic DNA as template. The primer pair PpATG11-BSD-F/PpATG11-BSD-R was used to amplify the blasticidin resistance gene using plasmid pPIC6A (Thermo Fisher Scientific, Waltham, MA, USA) as template. Using three fragments as the template, the primer pair EcoRI-PpATG11-1-F/BamHI-PpATG11-2-R was used to couple and amplify a 3.1 kb fragment by overlap PCR. This fragment was cloned into the EcoRI and BamHI sites of the vector pUC19 (Takara Bio, Otsu, Japan), yielding the *KpATG11* disruption vector pIS100. A deletion cassette for the *KpATG30* gene was constructed as follows: primer pairs HindIII-PpATG30-1-F/PpATG30-1-R and PpATG30-2-F/PstI-PpATG30-2-R were used to amplify 1.0 kb fragments using genomic DNA as template. The primer pair PpATG30-BSD-F/PpATG30-BSD-R was used to amplify the blasticidin resistance gene or zeocin resistance gene using plasmid pPIC6A or SK+Zeo^r, respectively. Using the three fragments as the template, the primer pair HindIII-PpATG30-1-F/PstI-PpATG30-2-R was used to couple and amplify a 3.1 kb fragment by overlap PCR. These fragments were cloned into the HindIII and PstI sites of the vector pIB1 (Takara Bio, Otsu, Japan), yielding the *ATG30* disruption vectors pOH104 and pOH105. For the *KpMPK1* deletion vector, primer pairs NotI-PpMPK1-1-F/KpnI-PpMPK1-1-R and SacI-PpMPK1-2-F/NotI-PpMPK1-2-R were used to amplify 1.0 kb fragments using genomic DNA as template. Using two fragments as the template, the primer pair KpnI-PpMPK1-1-R/SacI-PpMPK1-2-F was used to couple and amplify a 2.0 kb fragment by overlap PCR. This fragment was cloned into the KpnI and SacI sites of the vector SK+Zeo^r, yielding the *KpMPK1* disruption vector pIS101. Deletion cassettes for the *KpRLM1* and *KpSWI4* genes were constructed similarly. Primer pairs NotI-PpRLM1-1-F/KpnI-PpRLM1-1-R and SacI-PpRLM1-2-F/NotI-PpRLM1-2-R were used for the *KpRLM1* disruption vector pOH103. Primer pairs NotI-PpSWI4-1-F/KpnI-PpSWI4-1-R and SacI-PpSWI4-2-F/NotI-PpSWI4-2-R were used for the *KpSWI4* disruption vector pOH106. For the *KpMSG5* deletion vector, primer pairs PpMSG5-1-F/PpMSG5-1-R and PpMSG5-2-F/PpMSG5-2-R were used to amplify 1.0 kb fragments using genomic DNA as template. Primer pairs PpMSG5-ZEO-F/PpMSG5-ZEO-R were used to amplify the zeocin resistance gene using plasmid SK+Zeo^r. Using three fragments as the template, the primer pair PpMSG5-1-F/PpMSG5-2-R was used to couple and amplify a 3.1 kb fragment by overlap PCR. This fragment was ligated to Topo vector pCR2.1 (Thermo Fisher Scientific, Waltham, MA, USA), yielding the *KpMSG5* disruption vector pOH107. The deletion cassette for the *KpPTP2A* was constructed similarly. Primer pairs PpPTP2A-1-F/PpPTP2A-1-R, PpPTP2A-2-F/PpPTP2A-2-R and PpPTP2A-ZEO-F/PpPTP2A-ZEO-R were used to construct the *KpPTP2A* disruption vector pOH108. The deletion cassette using *ScARG4* as a marker for the *KpMSG5* was constructed similarly. Primer pairs PpMSG5-1-F/(ScArg4)-PpMSG5-1-R and (ScArg4)-PpMSG5-2-F/PpMSG5-2-R were used to amplify 1.0 kb fragments using genomic DNA as template, and (PpMSG5)-ScARG4-F/(PpMSG5)-ScARG4-R was used to amplify an *ScARG4* fragment using plasmid pSY8200 as template. Using three fragments as the template, the primer pair PpMSG5-1-F/PpMSG5-2-R was used to couple and amplify a 3.1 kb fragment by overlap PCR. This fragment was ligated to Topo vector pCR2.1, yielding the *KpMSG5* disruption vector using *ARG4* as a marker, pOH109.

pIS100 was digested with EcoRI/BamHI to disrupt the *KpATG11* gene, and pOH104 and pOH105 were digested with HindIII/PstI to disrupt *KpATG30.* In order to disrupt the *KpWSC1, KpMSG5* and *KpPTP2A* genes, each disruption vector – pOH100, pOH107 and pOH108, respectively – was digested with EcoRI. pIS101, pOH103 and pOH106 were digested with NotI to disrupt *KpMPK1*, *KpRLM1* and *KpSWI4.* These digested DNA fragments were used to transform *K. phaffii* by electroporation. Proper gene disruptions were confirmed using colony PCR.

The *KpATG30* promoter and its open reading frame (ORF) region without the STOP codon was amplified using primers XhoI-PpATG30-subclo-F/SphI-PpATG30-subclo-R with genomic DNA as template. The PCR fragment was cloned into the XhoI and SphI sites of the vector pSY006, resulting in pRN001. The primer pair KpnI-P_{ACT1}-F/SpeI-PpWSC1-subclo-R was used to amplify the *KpWSC1* gene fragment using plasmids pOH202, pOH208 and pOH209 as the template, and cloned into the KpnI and SpeI sites of pOH206, resulting in pOH213, pOH215 and pOH216, respectively. The primer pair KpnI-P_{ACT1}-F/SpeI- PpWSC1(310-316Δ)-R was used to amplify the *KpWSC1* gene fragment using plasmid pOH205 as the template. The PCR fragment was cloned into the KpnI and SpeI sites of pOH206, resulting in pOH214. The primer pair BamHI-P_{ACT1}-F/SpeI-PpWSC3-R was used to amplify the *KpWSC3* gene fragment using plasmid pOH203 as the template. The PCR fragment was cloned into the BamHI and SpeI sites of pNT206, resulting in pOH217. The *KpMPK1* promoter and ORF region without the STOP codon was amplified using primers XmaI-MPK1-F/(YFP)-PpMPK1-R, with genomic DNA as template. The YFP region for coupling the *KpMPK1* ORF was amplified using primers (PpMPK1)-YFP-F/BamHI-YFP-R, using plasmid pNT205 as the template. Using the two fragments as templates, the primer pair XmaI-MPK1-F/BamHI-YFP-R was used to couple and amplify by overlap PCR. This fragment was cloned into the XmaI and BamHI sites of pNT204, resulting in pIS001. pIS001 was subjected to site-directed mutagenesis using PpMPK1(T188AY190F)-F and PpMPK1(T188AY190F)-R primers. The resultant plasmid was designated pIS002.

Measurement of methanol in the medium

Aliquots of the culture medium were subjected to gas chromatography (GC) analysis. After removing yeast cells by centrifugation, 2 µl of the culture medium was injected onto a Porapak Q (Agilent technologies, Santa Clara, CA, USA) column. The injector temperature was 180°C. The detection temperature was held at 180°C for 4 min.

Western blotting

The samples for KpPex11–YFP cleavage assays were prepared from cells harvested at an $OD_{600\ nm}$ of 2.0. The cells were resuspended in 1 ml of solution I [0.2 M NaOH and 0.5% (v/v) 2-mercaptoethanol] and incubated on ice for 10 min, and then 0.1 ml of 100% (w/v) trichloroacetic acid (TCA) solution was added to the suspension. The lysates were subjected to centrifugation at 20,000 ***g*** at 4°C for 5 min. The supernatant was removed, and the pellet was resuspended in 1 ml of acetone by brief sonication. The obtained sample was subjected to centrifugation at 20,00 ***g*** at 4°C for 5 min, and the pellet was dried, dissolved in 80 µl of sample buffer [0.1 M Tris-HCl (pH 7.5), 2% (w/v) SDS, 1% (v/v) glycerol, 0.5% (v/v) 2-mercaptoethanol and 0.01% (w/v) Bromophenol Blue] by brief sonication, incubated at 65°C for 10 min, then subjected to centrifugation at 20,000 ***g*** for 1 min. A 5 µl volume of the supernatant was electrophoresed on a 10% SDS–PAGE gel.

To prepare samples for detection of phosphorylated KpAtg30–3×HA, harvested cells were suspended in lysis buffer [50 mM Tris-HCl pH 7.5, 50 mM NaCl, 0.1 mM EDTA, 0.1% Triton-X100, 10% (v/v) glycerol, 1 mM phenylmethylsulfonyl fluoride and EDTA-free complete protease inhibitor cocktail (Roche Diagnostics, Basel, Switzerland)] and then lysed using Multi-Beads Shocker (Yasui Kikai, Osaka, Japan). Cell extracts were subjected to centrifugation at 10,000 ***g*** for 5 min at 4°C to remove cell debris, dissolved in sample buffer (125 mM Tris-HCl pH 6.8, 4% SDS, 20% glycerol, a dash of Bromophenol Blue and 10% 2-mercaptoethanol) and boiled for 5 min. Each sample was electrophoresed on a 12% SDS–PAGE gel.

The proteins were transferred to a PVDF membrane using semidry blotting (ATTO, Tokyo, Japan). The blots were incubated overnight with anti-GFP antibody (JL-8; Clontech, Mountain View, CA, USA), anti-FLAG antibody (M2; Merck Millipore, Darmstadt, Germany), anti-HA antibody (F7; Santa Cruz Biotech, Dallas, TX, USA), anti-phospho-MAPK (Thr202/Tyr204; 20G11; Cell Signaling Technology, MA, USA) or anti-β-actin (ab8224; Abcam, Cambridge, UK) at a 1:1000 dilution in TBS-T [20 mM Tris, 0.1% (v/v) Tween 20, 0.8% (w/v) NaCl and 0.02% (w/v) KCl] buffer. The membranes were washed three times with TBS-T buffer and incubated with HRP-conjugated anti-mouse IgG (12-349; Merck Millipore, Darmstadt, Germany) or HRP-conjugated anti-rabbit IgG secondary antibodies (12-348; Merck Millipore) at a 1:10,000 dilution for 1 h. Finally, bound secondary antibodies were detected using Western Lightning (Perkin-Elmer Life Science, Waltham, MA, USA) and the signals were analyzed using a Light Capture system (ATTO, Tokyo, Japan).

Fluorescence observation

K. phaffii cells were grown in 5 ml of YPD medium to the stationary phase at 28°C. Subsequently, 30 µl of this culture was transferred into 5 ml of fresh YPD medium and the cells were grown at 28°C for 5 h. The culture was then harvested by centrifugation at 176 ***g*** for 5 min, then resuspended in methanol medium containing 0.93 µg/ml FM4-64 (Molecular Probes, Eugene, OR, USA) to label the vacuolar membrane and grown at 28°C for 24 h. The cells were harvested by centrifugation and stored on ice until observation. Observations were carried out using an IX81 fluorescence microscope (Olympus, Tokyo, Japan). Fluorescent images were captured with a charged coupled device (CCD) camera (SenSys; PhotoMetrics, Tucson, AZ, USA) using MetaMorph software (Universal Imaging, West Chester, PA, USA).

RNA isolation and reverse transcription quantitative PCR

A single colony was inoculated into YPD medium and cultivated overnight. Yeast cells were transferred into glucose medium to an $OD_{600\ nm}$ of 0.1 and cultivated to early exponential phase. The cells were shifted to methanol medium at an $OD_{600\ nm}$ of 1.0 and cultured at 28°C. Cells were harvested at the indicated time point by centrifugation at 10,000 ***g*** for 1 min at 4°C. The methods used for RNA extraction and reverse transcription were described previously (Ohsawa et al., 2017).

The quantitative real-time PCR was performed with a Light Cycler Instrument (Roche Diagnostics, Basel, Switzerland). The PCR reaction was performed with SYBR Premix Ex Taq (Takara) and the primers for *KpGAP1, KpMAG5* and *KpPTP2A* are listed in Table S3. The copy numbers of each sample were estimated using the Light Cycler software Version 4.1.

Acknowledgements

We are grateful to Professor Emeritus Teruhiko Beppu, University of Tokyo, and Professor Kenji Ueda, Nihon university, for their advice and technical information on using Beppu flasks. We also thank Tomoyuki Takeya and other Sakai laboratory members for helpful discussion and their technical assistance.

Competing interests

The authors declare no competing or financial interests.

Author contributions

Conceptualization: H.Y., Y.S.; Formal analysis: S.O., K.I., T.I.; Investigation: S.O., K.I., T.I.; Resources: Y.S.; Data curation: S.O., K.I., T.I., M.O., Y.S.; Writing - original draft: S.O., K.I., M.O., Y.S.; Writing - review & editing: S.O., M.O., H.Y., Y.S.; Supervision: M.O., H.Y., Y.S.; Project administration: Y.S.; Funding acquisition: M.O., H.Y., Y.S.

Funding

This research was supported by Grants-in-Aid for Scientific Research on Innovative Areas (16H0101200 and 19H05709 to Y.S.) from the Ministry of Education, Culture, Sports, Science and Technology, and by Grants-in-Aid for Scientific Research (B) (19H02870 to Y.S. and 16H02997 to H.Y.) and a Grant-in-Aid for Scientific Research (C) (20K05838 to M.O.) from the Japan Society for the Promotion of Science.

Peer review history

The peer review history is available online at https://journals.biologists.com/jcs/article-lookup/doi/10.1242/jcs.254714

References

Asakura, M., Ninomiya, S., Sugimoto, M., Oku, M., Yamashita, S., Okuno, T., Sakai, Y. and Takano, Y. (2009). Atg26-mediated pexophagy is required for host invasion by the plant pathogenic fungus Colletotrichum orbiculare. *Plant Cell* **21**, 1291-1304. doi:10.1105/tpc.108.060996

Burnett, S. F., Farré, J.-C., Nazarko, T. Y. and Subramani, S. (2015). Peroxisomal Pex3 activates selective autophagy of peroxisomes via interaction with the pexophagy receptor Atg30. *J. Biol. Chem.* **290**, 8623-8631. doi:10.1074/jbc.M114.619338

Dupres, V., Alsteens, D., Wilk, S., Hansen, B., Heinisch, J. J. and Dufrene, Y. F. (2009). The yeast Wsc1 cell surface sensor behaves like a nanospring in vivo. *Nat. Chem. Biol.* **5**, 857-862. doi:10.1038/nchembio.220

Farré, J.-C., Manjithaya, R., Mathewson, R. D. and Subramani, S. (2008). PpAtg30 tags peroxisomes for turnover by selective autophagy. *Dev. Cell* **14**, 365-376. doi:10.1016/j.devcel.2007.12.011

Farré, J.-C., Burkenroad, A., Burnett, S. F. and Subramani, S. (2013). Phosphorylation of mitophagy and pexophagy receptors coordinates their interaction with Atg8 and Atg11. *EMBO Rep.* **14**, 441-449. doi:10.1038/embor.2013.40

Irie, K., Takase, M., Lee, K. S., Levin, D. E., Araki, H., Matsumoto, K. and Oshima, Y. (1993). MKK1 and MKK2, which encode Saccharomyces cerevisiae mitogen-activated protein kinase-kinase homologs, function in the pathway mediated by protein kinase C. *Mol. Cell. Biol.* **13**, 3076-3083. doi:10.1128/MCB.13.5.3076

Kawaguchi, K., Yurimoto, H., Oku, M. and Sakai, Y. (2011). Yeast methylotrophy and autophagy in a methanol-oscillating environment on growing *Arabidopsis thaliana* leaves. *PLoS ONE* **6**, e25257. doi:10.1371/journal.pone.0025257

Lee, K. S., Irie, K., Gotoh, Y., Watanabe, Y., Araki, H., Nishida, E., Matsumoto, K. and Levin, D. E. (1993). A yeast mitogen-activated protein kinase homolog (Mpk1p) mediates signalling by protein kinase C. *Mol. Cell. Biol.* **13**, 3067-3075. doi:10.1128/MCB.13.5.3067

Levin, D. E. (2011). Regulation of cell wall biogenesis in Saccharomyces cerevisiae: the cell wall integrity signaling pathway. *Genetics* **189**, 1145-1175. doi:10.1534/genetics.111.128264

Lin-Cereghino, G. P., Godfrey, L., de la Cruz, B. J., Johnson, S., Khuongsathiene, S., Tolstorukov, I., Yan, M., Lin-Cereghino, J., Veenhuis, M., Subramani, S. et al. (2006). Mxr1p, a key regulator of the methanol utilization pathway and peroxisomal genes in *Pichia pastoris*. *Mol. Cell. Biol.* **26**, 883-897. doi:10.1128/MCB.26.3.883-897.2006

Lodder, A. L., Lee, T. K. and Ballester, R. (1999). Characterization of the Wsc1 protein, a putative receptor in the stress response of *Saccharomyces cerevisiae*. *Genetics* **152**, 1487-1499.

Manjithaya, R., Jain, S., Farré, J.-C. and Subramani, S. (2010). A yeast MAPK cascade regulates pexophagy but not other autophagy pathways. *J. Cell. Biol.* **189**, 303-310. doi:10.1083/jcb.200909154

Mao, K., Wang, K., Zhao, M., Xu, T. and Klionsky, D. J. (2011). Two MAPK-signaling pathways are required for mitophagy in *Saccharomyces cerevisiae*. *J. Cell Biol.* **193**, 755-767. doi:10.1083/jcb.201102092

Meijer, A. J. and Codogno, P. (2006). Signalling and autophagy regulation in health, aging and disease. *Mol. Aspects Med.* **27**, 411-425. doi:10.1016/j.mam.2006.08.002

Mizushima, N. and Komatsu, M. (2011). Autophagy: renovation of cells and tissues. *Cell* **147**, 728-741. doi:10.1016/j.cell.2011.10.026

Motley, A. M., Nuttall, J. M. and Hettema, E. H. (2012). Atg36: the *Saccharomyces cerevisiae* receptor for pexophagy. *Autophagy* **8**, 1680-1681. doi:10.4161/auto.21485

Nazarko, T. Y., Farré, J.-C. and Subramani, S. (2009). Peroxisome size provides insights into the function of autophagy-related proteins. *Mol. Biol. Cell* **20**, 3828-3839. doi:10.1091/mbc.e09-03-0221

Nazarko, T. Y., Ozeki, K., Till, A., Ramakrishnan, G., Lotfi, P., Yan, M. and Subramani, S. (2014). Peroxisomal Atg37 binds Atg30 or palmitoyl-CoA to regulate phagophore formation during pexophagy. *J. Cell Biol.* **204**, 541-557. doi:10.1083/jcb.201307050

Ohsawa, S., Yurimoto, H. and Sakai, Y. (2017). Novel function of Wsc proteins as a methanol-sensing machinery in the yeast *Pichia pastoris*. *Mol. Microbiol.* **104**, 349-363. doi:10.1111/mmi.13631

Ohsawa, S., Nishida, S., Oku, M., Sakai, Y. and Yurimoto, H. (2018). Ethanol represses the expression of methanol-inducible genes via acetyl-CoA synthesis in the yeast Komagataella phaffii. *Sci. Rep.* **8**, 18051. doi:10.1038/s41598-018-36732-2

Oku, M. and Sakai, Y. (2016). Pexophagy in yeasts. *Biochim. Biophys. Acta* **1863**, 992-998. doi:10.1016/j.bbamcr.2015.09.023

Oku, M., Takano, Y. and Sakai, Y. (2014). The emerging role of autophagy in peroxisome dynamics and lipid metabolism of phyllosphere microorganisms. *Front. Plant Sci.* **5**, 81. doi:10.3389/fpls.2014.00081

Pang, Y., Yamamoto, H., Sakamoto, H., Oku, M., Mutungi, J. K., Sahani, M. H., Kurikawa, Y., Kita, K., Noda, N. N., Sakai, Y. et al. (2019). Evolution from covalent conjugation to non-covalent interaction in the ubiquitin-like ATG12 system. *Nat. Struct. Mol. Biol.* **26**, 289-296. doi:10.1038/s41594-019-0204-3

Parua, P. K., Ryan, P. M., Trang, K. and Young, E. T. (2012). *Pichia pastoris* 14-3-3 regulates transcriptional activity of the methanol inducible transcription factor Mxr1 by direct interaction. *Mol. Microbiol.* **85**, 282-298. doi:10.1111/j.1365-2958.2012.08112.x

Rodicio, R. and Heinisch, J. J. (2010). Together we are strong–cell wall integrity sensors in yeasts. *Yeast* **27**, 531-540. doi:10.1002/yea.1785

Sahu, U., Krishna Rao, K. and Rangarajan, P. N. (2014). Trm1p, a Zn(II)(2)Cys(6)-type transcription factor, is essential for the transcriptional activation of genes of methanol utilization pathway, in *Pichia pastoris*. *Biochem. Biophys. Res. Commun.* **451**, 158-164. doi:10.1016/j.bbrc.2014.07.094

Sakai, Y., Koller, A., Rangell, L. K., Keller, G. A. and Subramani, S. (1998). Peroxisome degradation by microautophagy in *Pichia pastoris*: identification of specific steps and morphological intermediates. *J. Cell Biol.* **141**, 625-636. doi:10.1083/jcb.141.3.625

Takeya, T., Yurimoto, H. and Sakai, Y. (2018). A *Pichia pastoris* single-cell biosensor for detection of enzymatically produced methanol. *Appl. Microbiol. Biotechnol.* **102**, 7017-7027. doi:10.1007/s00253-018-9144-9

Tanaka, C., Tan, L.-J., Mochida, K., Kirisako, H., Koizumi, M., Asai, E., Sakoh-Nakatogawa, M., Ohsumi, Y. and Nakatogawa, H. (2014). Hrr25 triggers selective autophagy-related pathways by phosphorylating receptor proteins. *J. Cell Biol.* **207**, 91-105. doi:10.1083/jcb.201402128

Wang, X., Wang, Q., Wang, J., Bai, P., Shi, L., Shen, W., Zhou, M., Zhou, X., Zhang, Y. and Cai, M. (2016). Mit1 transcription factor mediates methanol signaling and regulates the alcohol oxidase 1 (AOX1) promoter in *Pichia pastoris*. *J. Biol. Chem.* **291**, 6245-6261. doi:10.1074/jbc.M115.692053

Watanabe, Y., Irie, K. and Matsumoto, K. (1995). Yeast RLM1 encodes a serum response factor-like protein that may function downstream of the Mpk1 (Slt2) mitogen-activated protein kinase pathway. *Mol. Cell. Biol.* **15**, 5740-5749. doi:10.1128/MCB.15.10.5740

Xie, Z. and Klionsky, D. J. (2007). Autophagosome formation: core machinery and adaptations. *Nat. Cell Biol.* **9**, 1102-1109. doi:10.1038/ncb1007-1102

Zientara-Rytter, K., Ozeki, K., Nazarko, T. Y. and Subramani, S. (2018). Pex3 and Atg37 compete to regulate the interaction between the pexophagy receptor, Atg30, and the Hrr25 kinase. *Autophagy* **14**, 368-384. doi:10.1080/15548627.2017.1413521

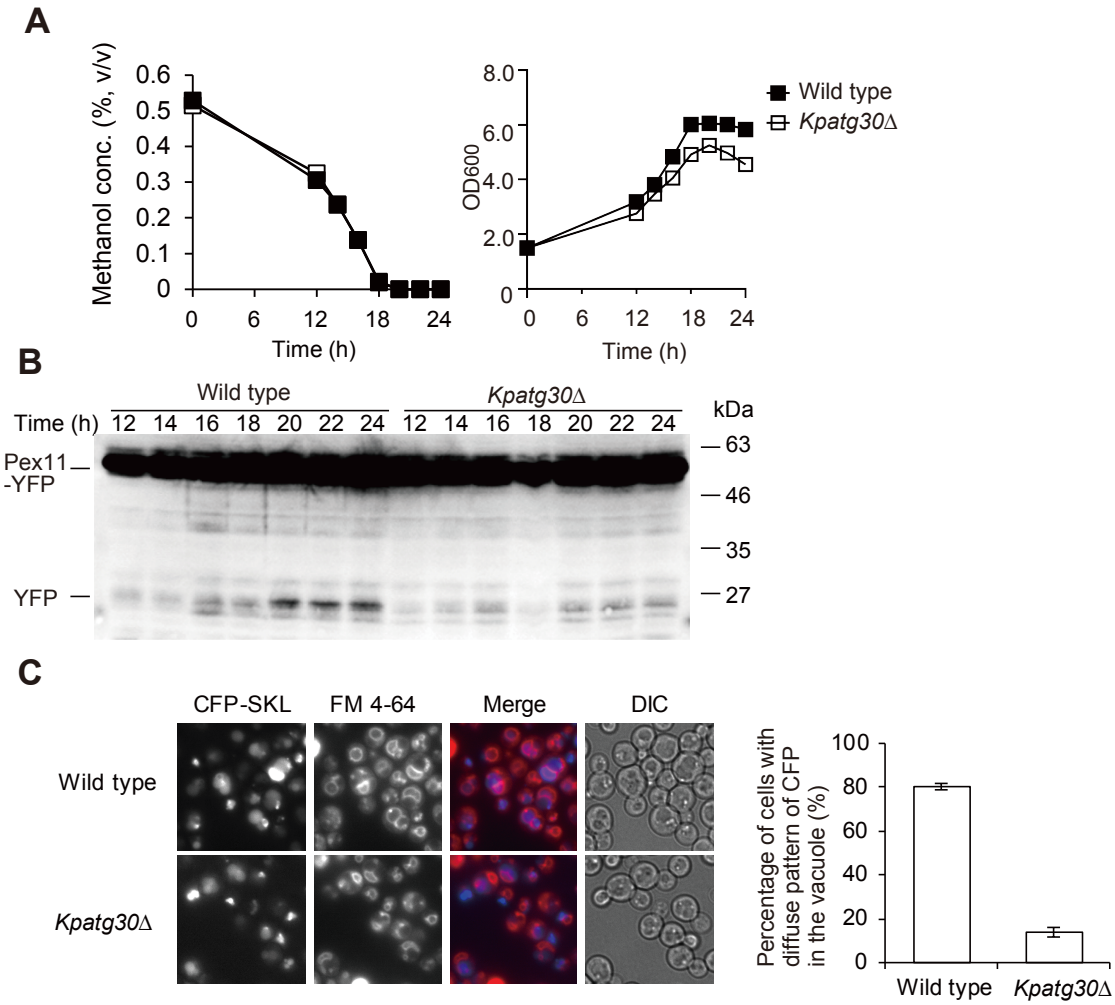

Fig. S1. Atg30-dependent pexophagy during methanol-consumption in batch-cultured growth. (A) Kinetics of methanol consumption (left) and growth of the wild-type and *Kpatg30*Δ strains (right) in 2 chambers of the *Beppu* flask. (B) Immunoblot analysis of KpPex11-YFP expressed in the wild-type and *Kpatg30*Δ strains. (C) Fluorescence microscopy of the wild-type and *Kpatg30*Δ cells with CFP-labeled peroxisomes (CFP-SKL) and FM4-64 -stained vacuolar membranes cultured on methanol-medium for 20 h in a *Beppu* flask. Brightfield images are shown as DIC. The graph shows the results of morphometric assays counting the percentage of the cells with CFP-SKL signal diffused in vacuole.

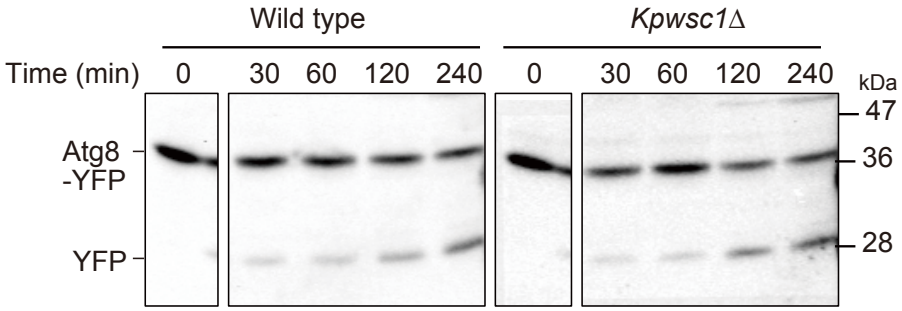

Fig. S2. Macropexophagy in *Kpwsc1*Δ strain. Immunoblot analysis of the lysates from the wild-type and *Kpwsc1*Δ strain expressing KpAtg8-YFP. The timepoints of sample acquisition after the shift from methanol medium to ethanol medium to induce macropexophagy are indicated. KpAtg8-YFP and cleavage YFP were detected using anti-GFP antibody.

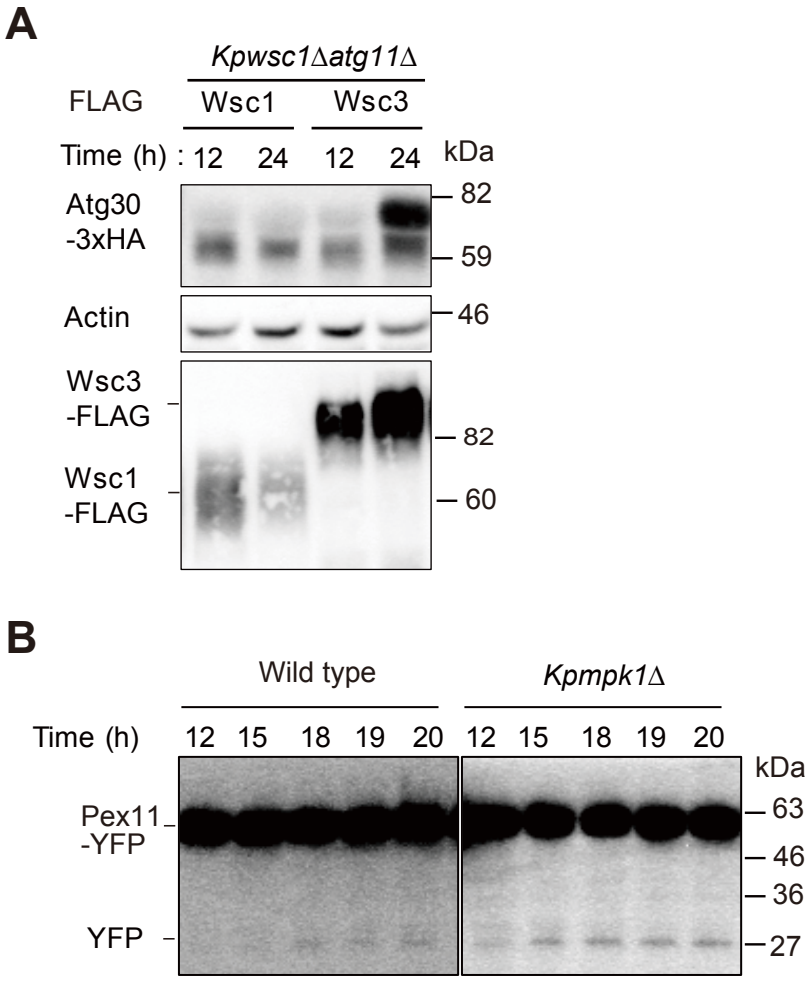

Fig. S3. Expression of KpWsc1-FLAG and KpWsc3-FLAG in *Kpwsc1*Δ*atg11*Δ strain, and pexophagy in *Kpmpk1*Δ strain. (A) Immunoblot analysis of the lysates from the *Kpwsc1*Δ*atg11*Δ strain expressing either KpWsc1-FLAG (KpWsc1) or KpWsc3-FLAG (KpWsc3). The timepoints of sample acquisition after the start of methanol culture are indicated. KpWsc1-FLAG and KpWsc3-FLAG bands were detected using anti-FLAG antibody reactive to FLAG. (B) Immunoblot analysis of Pex11-YFP expressed in the wild-type and *Kpmpk1*Δ strains cultured in a *Beppu* flask, as described in legend to Fig. 1.

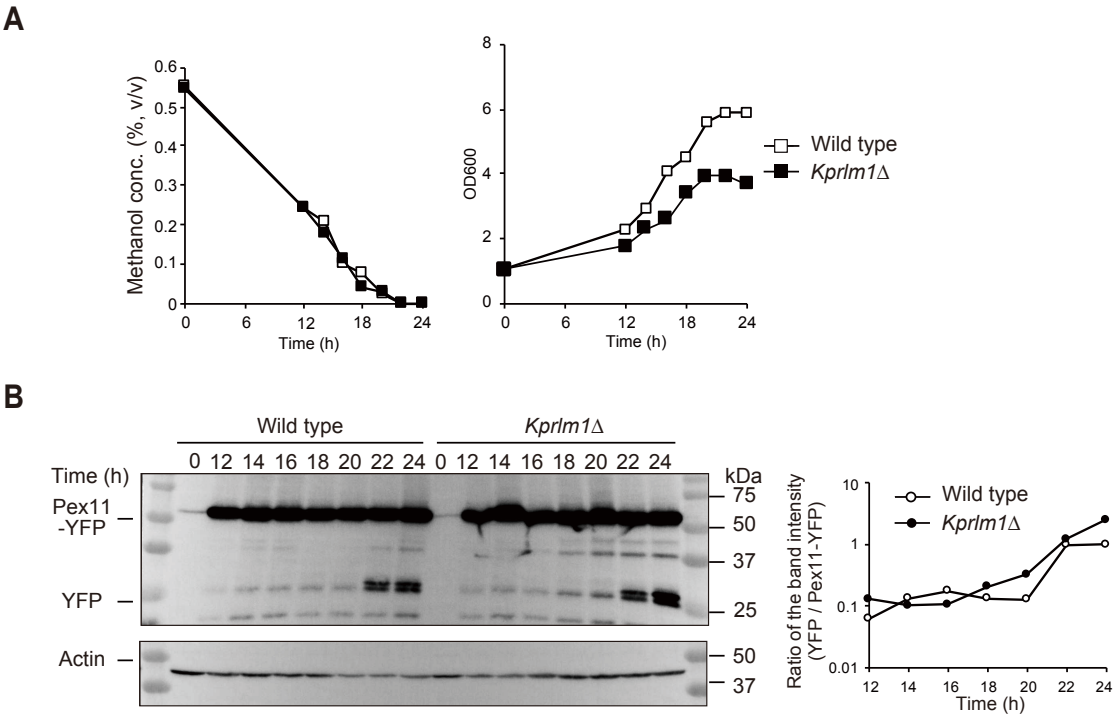

Fig. S4. Onset of pexophagy in the *rlm1*Δ strain during batch culture on methanol in a *Beppu* flask. (A) Kinetics of methanol consumption (left) and growth of the wild-type and *Kprlm1*Δ strains (right) in 2 chambers of the *Beppu* flask. (B) (Left panel) Immunoblot analysis of KpPex11-YFP expressed in the wild-type and *Kprlm1*Δ strains. (Right panel) Quantitative analysis of YFP-band intensity relative to KpPex11-YFP band intensity.

Table S1. Yeast strains used in this study

Strain	Genotype	Reference
PPY12	*Kparg4 Kphis4* (parental strain)	Sakai *et al.* (1998)
GS115	*Kphis4*	Cregg *et al*. (1985)
OH2002	GS115, *Kphis4*::(P_{KpACT1}*KpATG30-3xHA*)	This study
IS20000	PPY12, P_{PEX11}*KpPex11-YFP::KpARG4*	This study
IS20009	IS20000, *Kphis4::KpHIS4* $P_{KpPEX11}$*KpPEX11-YFP::KpARG4*	This study
IS20010	IS20009, *Kpatg30*::*Zeo*^{r}	This study
IS20011	IS20009, *Kpwsc1*::*Zeo*^{r}	This study
IS20012	IS20009*, Pprlm1::Zeor*	This study
IS10020	GS115, P_{KpAOX1}*CFP-SKL::KpHIS4*	This study
IS17020	IS10020, *Kpatg30::BSD*	This study
IS20110	PPY12, *Kpatg11:: BSD*, $P_{KpATG30}$*KpATG30-3xHA:: KpHIS4*	This study
IS20111	IS20110, *Kparg4::KpARG4*	This study
IS24110	IS20110, *Kpwsc1::Zeo*^{r}	This study
IS24111	IS24110, *Kparg4::KpARG4*	This study
IS24112	IS24110, P_{KpACT1}*KpWSC1-5xFLAG::KpARG4*	This study
IS24113	IS24110, P_{KpACT1}*KpWSC1(310-316Δ)-5xFLAG::KpARG4*	This study
IS24116	IS24110, P_{KpACT1}*KpWSC1(Y53A)-5xFLAG::KpARG4*	This study
IS24117	IS24110, P_{KpACT1}*KpWSC1(Y53F)-5xFLAG::KpARG4*	This study
IS22110	IS20110, *Kpmpk1::Zeo*^{r}	This study
IS22111	IS22110, *Kparg4::KpARG4*	This study
IS22112	IS22110, P_{KpMPK1}*KpMPK1-YFP::KpARG4*	This study
IS22113	IS22110, P_{KpMPK1}*KpMPK1(TAYF)-YFP::KpARG4*	This study
IS23110	IS20110, *Kprlm1::Zeo*^{r}	This study
IS23111	IS23110, *Kparg4::KpARG4*	This study
IS23116	IS20110, *Kpswi4::Zeo*^{r}	This study
IS23117	IS23116, *Kparg4::KpARG4*	This study
IS23118	IS20110, *Kpmsg5::Zeo*^{r}	This study
IS23119	IS23118, *Kparg4::KpARG4*	This study
IS23120	IS20110, *Kpptp2a::Zeo*^{r}	This study
IS23121	IS23120, *Kparg4::KpARG4*	This study
IS23122	IS23120, *Kpmsg5::KpARG4*	This study
IS24118	IS24110, P_{KpACT1}*KpWSC3-5xFLAG::KpARG4*	This study
SA1017	PPY12*, arg4::pSAP115(PATG8YFP-PpATG8, ARG4)*	Mukaiyama et al. (2004)
IS24119	SA1017, *his4*::*HIS4*	This study
IS24120	SA1017*, Ppwsc1::Zeor*	This study
IS24121	IS24120*, his4::HIS4*	This study

Table S2. Plasmids used in this study

Designation	Discription	Reference
pIB1	*KpHIS4*	Sears *et al*. (1998)
SK+Zeo^r	Zeo^r	Yano *et al*. (2009)
pOH100	Δ*Kpwsc1::Zeo^r*	Ohsawa *et al.* (2017)
pOH103	Δ*Kprlm1::Zeo^r*	This study
pOH104	*ΔKpatg30::Bsd^r*	This study
pOH105	Δ*Kpatg30::Zeo^r*	This study
pOH106	Δ*Kpswi4::Zeo^r*	This study
pOH107	Δ*Kpmsg5*Δ*::Zeo^r*	This study
pOH108	Δ*Kpptp2a*Δ*::Zeo^r*	This study
pOH109	Δ*Kpmsg5*Δ*::ScARG4*	This study
pIS100	*ΔKpatg11::Bsd^r*	This study
pIS101	*ΔKpmpk1::Zeo^r*	This study
pSY302	$P_{KpPEX11}$*KpPEX11-YFP KpARG4*	Laboratory collection
pSY8200	pIB1 *KpHIS4::ScARG4*	Ohsawa *et al.* (2017)
pSY006	pIB1 3xHA *KpHIS4*	Ohsawa *et al.* (2017)
pRN001	$P_{KpATG30}$*KpATG30-3xHA KpHIS4*	This study
pYA006	P_{KpAOX1}*CFP-SKL KpHIS4*	Ano *et al.* (2005)
pOH202	P_{KpACT1}*KpWSC1-3xHA KpHIS4*	Ohsawa *et al.* (2017)
pOH203	P_{KpACT1}*KpWSC3-3xHA KpHIS4*	Ohsawa *et al.* (2017)
pOH205	P_{KpACT1}*KpWSC1(310-316*Δ*)-3xHA KpHIS4*	Ohsawa *et al.* (2017)
pOH208	P_{KpACT1}*KpWSC1(Y53A)-3xHA KpHIS4*	Ohsawa *et al.* (2017)
pOH209	P_{KpACT1}*KpWSC1(Y53F)-3xHA KpHIS4*	Ohsawa *et al.* (2017)
pNT206	pIB1 5xFLAG *KpARG4*	Tamura *et al.* (2013)
pOH213	P_{KpACT1}*KpWSC1-5xFLAG KpARG4*	This study
pOH214	P_{KpACT1}*KpWSC1(310-316*Δ*)-5xFLAG KpARG4*	This study
pOH215	P_{KpACT1}*KpWSC1(Y53A)-5xFLAG KpARG4*	This study
pOH216	P_{KpACT1}*KpWSC1(Y53F)-5xFLAG KpARG4*	This study
pOH217	P_{KpACT1}*KpWSC3-5xFLAG KpARG4*	This study
pNT204	pIB1 *KpARG4*	Tamura *et al.* (2010)
pNT205	YFP-pIB1 *KpARG4*	Tamura *et al.* (2010)
pIS001	P_{KpMPK1}*KpMPK1-YFP KpARG4*	This study
pIS002	P_{KpMPK1}*KpMPK1(TAYF)-YFP KpARG4*	This study

Table S3. Primers used in this study

Designation	DNA Sequence
PpATG11-BSD-F	5'-GGATCTCAACAAACTGCGGTAGCCCACACACCATAGCTTC-3'
PpATG11-BSD-R	5'-CAGTCCATCGATCTCCGTTTTTGTAATAGAACAAGAAAAATGAAACTGA-3'
EcoRI-PpATG11-1-F	5'-CGGAATTCAACGCAACACAAGTCCTTCC-3'
PpATG11-1-R	5'-GAAGCTATGGTGTGTGGGCTACCGCAGTTTGTTGAGATCC-3'
PpATG11-2-F	5'-TCAGTTTCATTTTTCTTGTTCTATTACAAAAACGGAGATCGATGGACTG-3'
BamHI-PpATG11-2-R	5'-CGGGATCCGGAGACGACACCACATTGAA-3'
HindIII-PpATG30-1-F	5'-CCCAAGCTTTGCCATTTAGCTCCCTGATT-3'
PpATG30-1-R	5'-GAAGCTATGGTGTGTGGGCTATATTCTTGCTCGGCATCGT-3'
PpATG30-2-F	5'-CGAAGGCTTTAATTTGCAAGCTCCAATTCCCAGTCCACATCT-3'
PstI-PpATG30-2-R	5'-TGCACTGCAGTGCCAAGTCTGACTCCCTTT-3'
PpATG30-BSD-F	5'-ACGATGCCGAGCAAGAATATAGCCCACACACCATAGCTTC-3'
PpATG30-BSD-R	5'-AGATGTGGACTGGGAATTGGAGCTTGCAAATTAAAGCCTTCG-3'
NotI-PpMPK1-1-F	5'-CGATTATTTCTTCGGTGCCTGCGGCCGCCCTGAAGAGGGGAAAGAAGG-3'
KpnI-PpMPK1-1-R	5'-GGGGTACCCACCTTTTTGATGGCCACTT-3'
SacI-PpMPK1-2-F	5'-CCCGAGCTCCGGATTGGATCGGTATGGTA-3'
NotI-PpMPK1-2-R	5'-CCTTCTTTCCCCTCTTCAGGGCGGCCGCAGGCACCGAAGAAATAATCG-3'
NotI-PpRLM1-1-F	5'-ATTGCCAGAAAGCAACGTCTGCGGCCGCAACTCATCAGGCGTGCTTTT-3'
KpnI-PpRLM1-1-R	5'-GGGGTACCAAAGCCCAGCTTTCCTCTTC-3'
SacI-PpRLM1-2-F	5'-CCCGAGCTCCGAGATTTCCAAGCAGTGTG-3'
NotI-PpRLM1-2-R	5'-AAAAGCACGCCTGATGAGTTGCGGCCGCAGACGTTGCTTTCTGGCAAT-3'
NotI-PpSWI4-1-F	5'-GAGTGGACGTCAGCATTTCAGCGGCCGCGGAGCATCGAGTGTGTTGTG-3'
KpnI-PpSWI4-1-R	5'-GGGGTACCACCTCCTTGGATCCTCTGGT-3'
SacI-PpSWI4-2-F	5'-CCCGAGCTCCGCATGAAGCTGGTAAATGA-3'
NotI-PpSWI4-2-R	5'-CACAACACACTCGATGCTCCGCGGCCGCTGAAATGCTGACGTCCACTC-3'
PpMSG5-1-F	5'-GACCAAAGACGTGGGAAGAA-3'
PpMSG5-1-R	5'-TTTGAAGCTATGGTGTGTGGGCGGTTCTTCTTCGAAACCTG-3'
PpMSG5-2-F	5'-CGAAGGCTTTAATTTGCAAGCTATCAGCCTACCTGCATCACC-3'
PpMSG5-2-R	5'-TACGTTTGGCATCTGGAGTG-3'
PpMSG5-ZEO-F	5'-CAGGTTTCGAAGAAGAACCGCCCACACACCATAGCTTCAAA-3'
PpMSG5-ZEO-R	5'-GGTGATGCAGGTAGGCTGATAGCTTGCAAATTAAAGCCTTCG-3'
PpPTP2A-1-F	5'-GTTTGGGGGCTACAACTTGA-3'
PpPTP2A-1-R	5'-TTTGAAGCTATGGTGTGTGGGCGAGATTCCTCGTACGCATT-3'
PpPTP2A-2-F	5'-CGAAGGCTTTAATTTGCAAGCTCGAAGACTCAGGGTATCAATGG-3'
PpPTP2A-2-R	5'-TCTTCGCTGTTCGTCTACCC-3'

PpPTP2A-ZEO-F	5'-AATGCGTACGAGGAATCTCGCCCACACACCATAGCTTCAAA-3'
PpPTP2A-ZEO-R	5'-CCATTGATACCCTGAGTCTTCGAGCTTGCAAATTAAAGCCTTCG-3'
(PpMSG5)-ScARG4-F	5'-CAGGTTTCGAAGAAGAACCGGATCTGCCAAGGCTCCATCA-3'
(PpMSG5)-ScARG4-R	5'-GGTGATGCAGGTAGGCTGATTATAAACTAAGACAACTGCTAAGTTGGTTAAC-3'
(ScArg4)-PpMSG5-1-R	5'-TGATGGAGCCTTGGCAGATCCGGTTCTTCTTCGAAACCTG-3'
(ScArg4)-PpMSG5-2-F	5'-GTTAACCAACTTAGCAGTTGTCTTAGTTTATAATCAGCCTACCTGCATCACC-3'
XhoI-PpATG30-subclo-F	5'-CCGCTCGAGGGCGATGAGAGGAAGCATTA-3'
SphI-PpATG30-subclo-R	5'-ACATGCATGCTAAAATCTCCTGTTTGAGCTTTGA-3'
KpnI-P_{ACTI}-F	5'-GGGGTACCTCGCTGGTAATCCCGGCT-3'
SpeI-PpWSC1-subclo-R	5'-GGACTAGTAGCATCATCAGGATTTGCTACC-3'
SpeI-PpWSC1(310-316Δ)-R	5'-GGACTAGTAGCATCCACCTTCCTGGAGTAATCTGCT-3'
BamHI-P_{ACTI}-F	5'-CGGGATCCTCGCTGGTAATCCCGGCT-3'
SpeI-PpWSC3-R	5'-GGACTAGTAACTTCATCATCTGTGGGGTT-3'
XmaI-MPK1-F	5'-TTCCCCCCGGGTCGAGAAAACGCAAACTCTG-3'
(YFP)-PpMPK1-R	5'-CATGCCTGCAGCTCGAGCTGTGTACCATACCGATCCAATC-3'
(PpMPK1)-YFP-F	5'-GATTGGATCGGTATGGTACACAGCTCGAGCTGCAGGCATG-3'
BamHI-YFP-R	5'-CGCGGATCCTTACTTGTACAGCTCGTCCATGC-3'
PpMPK1(T188AY190F)-F	5'-TTTCTTGCTGAATTTGTTGCTACCAGGTGGTAT-3'
PpMPK1(T188AY190F)-R	5'-AGCAACAAATTCAGCAAGAAAGCCAGCATTCTT-3'
RT-GAP1-F	5'-CCACCGGTGTTTTCACCACT-3'
RT-GAP1-R	5'-CACCGACAACGAACATTGGA-3'
RT-PpMSG5-F	5'-ACCGATCCCGGAATACCAAG-3'
RT-PpMSG5-R	5'-TCCAGTTCTGTGGCGGACTT-3'
RT-PpPTP2A-F	5'-TGGCTTCTCCTGGATGTGGT-3'
RT-PpPTP2A-R	5'-GGTCTTTGGCACTTGCTGCT-3'

Table S4: Supplementary Figure 1C cell count

Click here to download Table S4